JOURNAL OF COMPUTATIONAL PHYSICS **102**, 417–422 (1992)

NOTE

Comparison between 1 D and $1\frac{1}{2}$D Eulerian Vlasov Codes for the Numerical Simulation of Stimulated Raman Scattering

1. INTRODUCTION

Recently, a relativistic Eulerian Vlasov code has been developed to study charged particle acceleration through stimulated Raman scattering or beat wave of intense laser beams in a plasma [1–3]. Most of the numerical studies on the topic were performed until recently with particle codes [4–6]. We have shown that the use of an eulerian scheme for the integration of the relativistic Vlasov equation allows a finer resolution in phase space than a particle code and especially provides a detailed examination of the low density regions of phase space which are badly delineated in the usual particle-in-cell (PIC) codes.

Since particle acceleration is achieved through a mechanism producing a longitudinal large amplitude electron plasma wave along the laser wave-vector direction (say x-direction) the relativistic Vlasov equation can be solved for the electron distribution $F(x, \mathbf{p}, t)$ only, together with Maxwell's equations, where all field quantities are functions of the space variable x only. Furthermore, we considered in [1–3] the following class of exact solution

$$F(x, \mathbf{p}, t) = \delta(\mathbf{p}_\perp - e\mathbf{A}_\perp)\, f(x, p_x, t)$$

which means that the longitudinal motion obeys the relativistic Vlasov equation for $f(x, p_x, t)$ which describes accurately the longitudinal motion of electrons in the two-dimensional $x - p_x$ phase space. On the other hand, the effective transverse motion of particles is "cold" and simply described by a fluid macroscopic equation for the transverse non-relativistic mean velocity $\mathbf{u}_\perp = e\mathbf{A}_\perp/m$, $\mathbf{A}_\perp$ being the transverse vector potential. Therefore the resulting Vlasov code has been called a "1D code" throughout this paper.

While restricted to a spatially periodic condition in [1], the code has been successfully extended to a nonperiodic causal bounded system [2, 3], allowing the code to deal with more realistic and longer plasmas.

The central goal of this paper is to answer the question whether the simplified macroscopic perpendicular description is adequate, especially for the strongly accelerated particle dynamics. This task has been achieved by extending our 1D Vlasov code into a full kinetic $1\frac{1}{2}$D code.

In Section 2 we present the numerical scheme for the electron distribtion function $f(x, p_x, v_y, t)$ in a three-dimensional phase space. The basic numerical steps are unchanged: the problems are only associated with memory size and CPU time. Comparison between 1D and $1\frac{1}{2}$D codes are presented in Section 3, for the Raman back-scattering case.

2. A PERIODIC RELATIVISTIC $1\frac{1}{2}$D EULER–VLASOV CODE

We consider an infinite homogeneous plasma with a laser wave-vector in the x-direction, an electromagnetic field E_y in the y-direction and B_z in the z-direction, all field quantities being functions of the space variable x only (see [1]). The electron distribution function $f(x, p_x, v_y, t)$ obeys the Vlasov equation

$$\frac{\partial f}{\partial t} + \frac{p_x}{m\gamma}\frac{\partial f}{\partial x} - e(E_x + v_y B_z)\frac{\partial f}{\partial p_x} - \frac{e}{m\gamma}\left(E_y - \frac{p_x}{m\gamma} B_z\right)\frac{\partial f}{\partial v_y} = 0, \tag{1}$$

where the Lorentz factor is given by

$$\gamma = \left(1 + \frac{p_x^2}{m^2c^2}\right)^{1/2} \tag{2}$$

assuming that $v_y \ll c$ in the transverse direction.

The longitudinal self-consistent electric field is given by Poisson's equation

$$\frac{\partial^2 \phi}{\partial x^2} + \frac{e}{\varepsilon_0}(n_i - n_e(x, t)) = 0, \tag{3}$$

with

$$E_x = -\partial\phi/\partial x, \tag{4}$$

n_i being the homogeneous ion density and n_e the electron density defined by

$$n_e = \int f(x, p_x, v_y, t)\, dp_x\, dv_y. \tag{5}$$

581/102/2-13

0021-9991/92 $5.00

The transverse electromagnetic fields obey Maxwell's equations,

$$\frac{\partial B_z}{\partial t} = -\frac{\partial E_y}{\partial x} \tag{6}$$

$$\frac{\partial E_y}{\partial t} = -c^2 \frac{\partial B_z}{\partial x} - \frac{J_y}{\varepsilon_0} \tag{7}$$

with

$$J_y(x, t) = -e \int v_y f(x, p_x, v_y, t)\, dp_x\, dv_y. \tag{8}$$

Numerical integration of Eq. (1) is obtained by using a well-known fractional step or splitting scheme. The scheme

$$\frac{\hat{H}}{2} \frac{\hat{V}_y}{2} \hat{P}_x \frac{\hat{V}_y}{2} \frac{\hat{H}}{2} \tag{9}$$

integrates the Vlasov equation over a full time step Δt with second-order accuracy. The operators $\hat{H}$, $\hat{V}_y$, and $\hat{P}_x$ denote respectively the shift of the electron distribution function in x, v_y, and p_x-directions for a time step Δt. Let us define $t_n = n\,\Delta t$ and $t_{n+1} = (n+1)\,\Delta t$ and $t_{n+1/2} = (n+\frac{1}{2})\,\Delta t$; thus the fractional step method involves five successive steps:

Step 1. $\hat{H}/2$ operator corresponds to the shift in the x-direction for a half time step $\Delta t/2$:

$$f^*(x, p_x, v_y, t_{n+1/2}) = f\left(x - \frac{p_x \Delta t}{2m\gamma}, p_x, v_y, t_n\right). \tag{10}$$

Step 2. $\hat{V}_y/2$ operator corresponds to the shift of the distribution function in the v_y-direction for a half time step $\Delta t/2$ and we have

$$f^{**}(x, p_x, v_y, t_{n+1/2}) = f^*\left(x, p_x, v_y + \frac{e}{m\gamma}\left(E_y - \frac{p_x}{m\gamma} B_z\right)\frac{\Delta t}{2}, t_{n+1/2}\right). \tag{11}$$

Step 3. $\hat{P}_x$ operator corresponds to the shift in the p_x-space for a full time step Δt, and we have

$$f^{***}(x, p_x, v_y, t_{n+1/2}) = f^{**}(x, p_x + e(E_x + v_y B_z)\,\Delta t, v_y, t_{n+1/2}). \tag{12}$$

and so on. Thus the sequence (9) allows us to compute f at grid points at time t_{n+1} from the known values at time t_n. A cubic spline interpolation is used to compute the various shifts of the distribution function; as in Ref. [1], spatially periodic boundary conditions are considered.

2. NUMERICAL RESULTS

A backward Raman scattering instability (BRS) has been investigated with the decay of an incident linearly polarized light with a wave number $k_0 = 3\,\Delta k = 2.1135\omega_p/c$ into a scattered electromagnetic wave $k_s = -\Delta k = -0.7045\omega_p/c$ and an electron plasma wave of wavenumber $k_e = 4\,\Delta k = 2.818\omega_p/c$ with the matching conditions $k_0 = k_s + k_e$ and $\omega_0 = \omega_e + \omega_s$ for the corresponding frequencies. $\Delta k = 2\pi/L$ is the fundamental mode, with L the length of the periodic box (in the present example we have $L = 8.919c/\omega_p$). These parameters are the same as in Section 4 of Ref. [1]. We have $\omega_e = (\omega_p^2 + 3k_e^2 v_{th}^2)^{1/2} = 1.073\omega_p$ for a corresponding value of the thermal longitudinal velocity $v_{th} = 0.08c$, and we have $\omega_0 = (\omega_p^2 + k_0^2 c^2)^{1/2} = 2.339\omega_p$ for the pump frequency.

The transverse thermal velocity is $v_{ty} = 0.06c$. Furthermore, for the mode k_s, the exact frequency would be $\omega = (\omega_p^2 + k_s^2 c^2)^{1/2} = 1.223\omega_p$ and therefore the frequency mismatch is $\Delta\omega = \omega_s - (\omega_0 - \omega_e) = -0.04\omega_p$. The initial condition for the electron distribution function is

$$f(x, p_x, v_y, t=0) = \frac{1}{2\pi v_{ty} v_{th}} e^{-(1/2v_{th}^2)(p_x - \alpha \cos k_e x)^2} + e^{-(1/2v_{ty}^2)(v_y - u_y^*(x))^2}. \tag{13}$$

This distribution function is a Maxwellian both in p_x and v_y space. In the exponent of Eq. (13), $\alpha \cos k_e x$ is a small initial perturbation to initiate BRS instability (we take $\alpha = 0.1$); $u_y(x)$ is the mean transverse velocity. With an initial (pump) electromagnetic wave $E_y = E_0 \cos k_0 x$, the corresponding value of u_y at time $t = 0$ is then $u_y = -v_{\text{osc}} \sin k_x x$. As in Ref. [1, Section 4], we select a quiver velocity $v_{\text{osc}}/c = 0.108$ ($n_0 = 0.18 n_{\text{crit}}$). Due to the centered character of our numerical scheme (10)–(12), $u_y^* = u_y$ ($t = -\Delta t/2$) has to be considered in the initial distribution function. This initialization respects the centered character of the numerical scheme. Other numerical parameters are identical as those used in Ref. [1, Section 4]. For the $1\frac{1}{2}$D model we have used a grid of $N_x N_{px} N_{v_y} = 64 \times 128 \times 64$ points. For the 1D model, we have used $N_x N_{px} = 64 \times 256$ points. The computation time for the $1\frac{1}{2}$D code was 2.5 μs per time step per grid point, and for the 1D code the computation time was 1.1 μs per time step per grid point. The error in the density conservation in both codes is 10^{-5}, and for the energy conservation it is 4×10^{-3}.

Figures 1, 2, and 3 show respectively the different energies in mc^2 units as function of time: the pump electromagnetic energy (mode k_0) and the electromagnetic scattered energy (mode k_s) and the electrostatic plasma field energy (mode k_e) are calculated respectively by using the 1D fluid Vlasov model in curves (a) and the $1\frac{1}{2}$D version in curves (b). In both cases the curves exhibit the same behavior in which the energy is transferred back and forth between the pump,

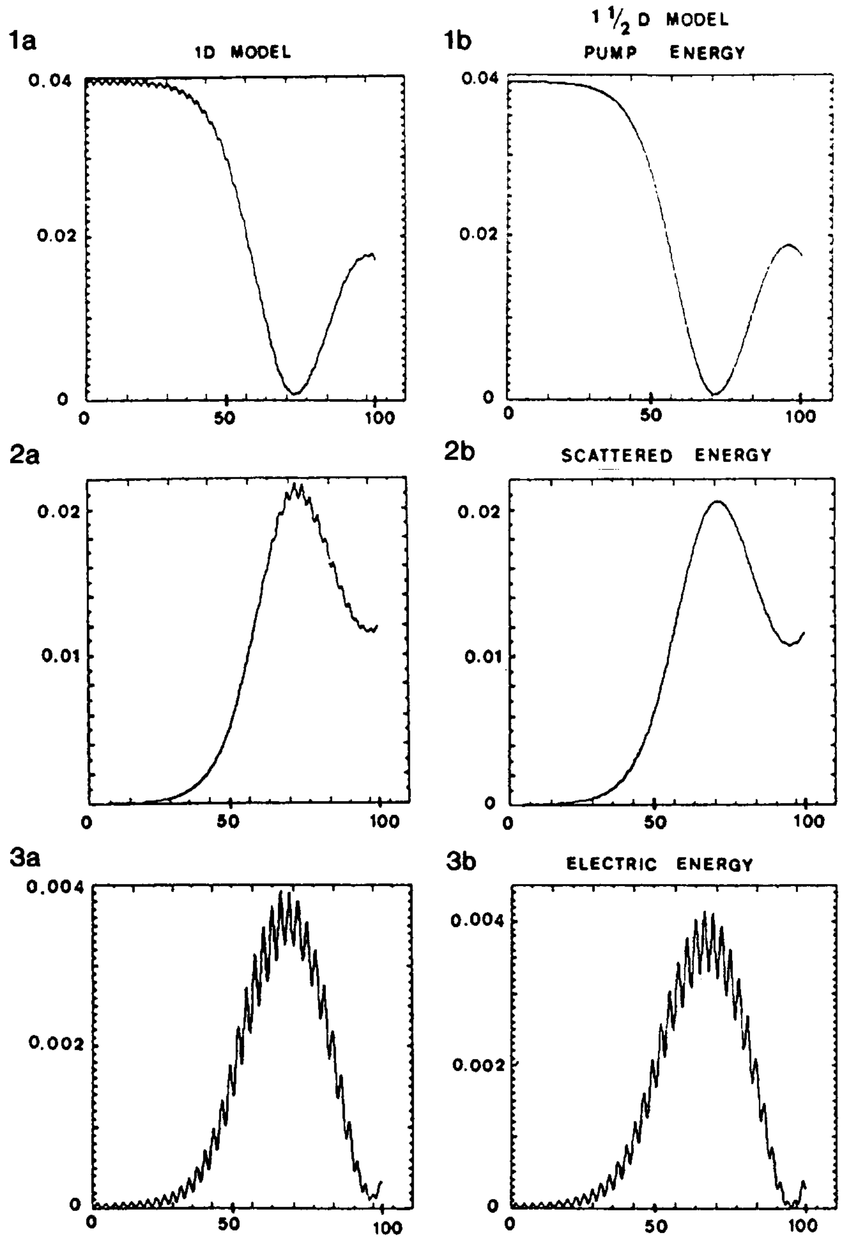

FIGS. 1–3. Time evolution for (1) the pump, (2) the scattered mode, and (3) the plasma mode for each (a) 1D model and each (b) $1\frac{1}{2}$D model.

scattered, and plasma waves. The detailed mechanism of particle trapping and acceleration can be observed in Fig. 4 in the $x-p_x$ phase space representation. Figure 4a shows contour-plots in the upper half phase place ($p_x > 0$) at three times: $t\omega_p = 40$, $t\omega_p = 50$, and $t\omega_p = 60$ for the 1D model, while Fig. 4b comes from the $1\frac{1}{2}$D kinetic code at the same times. Again numerical results are in good agreement; both curves show clearly the same particle acceleration process to high energies.

Furthermore, the $1\frac{1}{2}$D Euler–Vlasov code affords the required resolution to discern these phenomena and also the dynamics in the perpendicular phase-space as we can see in Figs. 5 and 6 at two different times during evolution. The first curve (Fig. 5a) gives, at time $t\omega_p = 30$, the representation of the distribution function (averaged over p_x variable) in the $x-v_y$ phase-space and the corresponding mean velocity $u_y(x)$ is shown in Fig. 5b, computed directly by averaging over v_y space the distribution function given in Fig. 5a.

Fig. 5c shows the corresponding mean velocity computed in the 1D model at the same time. Other curves of Figs. 6a, b, and c are related to time $t\omega_p = 70$. Two points must be pointed out:

— First, the modulation of the electron distribution function, initially on the mode $k_0 = 3\,\Delta k$ (due to the pump

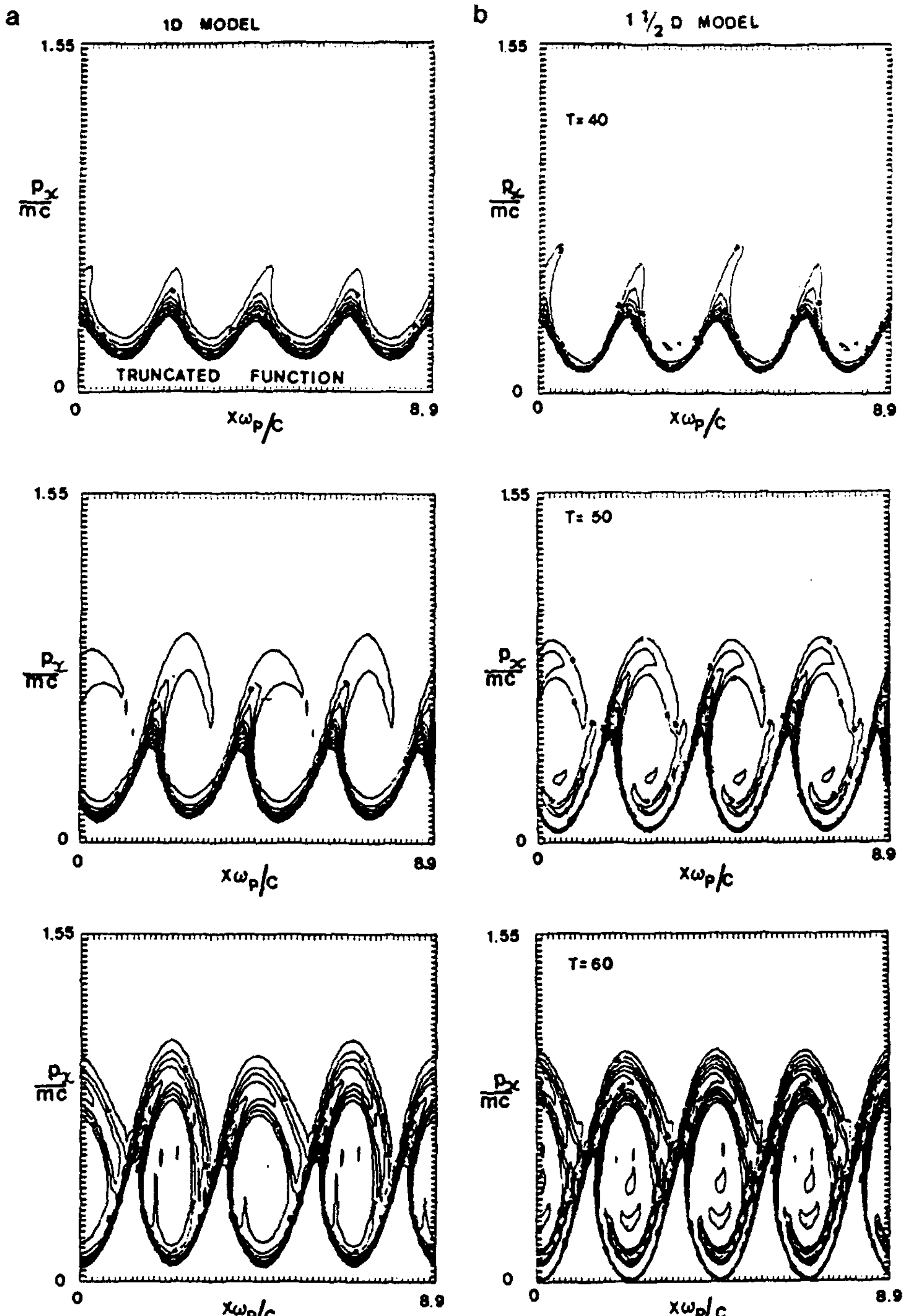

FIG. 4. Comparison of the phase-space $p_x - x$ contour plots for the 1D and $1\frac{1}{2}$D models.

electromagnetic wave) evolves according to the matching condition $k_0 = k_e + k_s$ to end up with a modulation on the mode $|k_s| = \Delta k$ at the time $t\omega_p = 70$, corresponding to the scattered light wavenumber.

— Second, a modulation on the plasma mode $k_e = 4\,\Delta k$, acting on the bulk of the distribution function can be viewed in Fig. 5a, during the growth of the electron plasma wave.

On the other hand, we have represented in Figs. 7a and b the contour-plots in the upper half space ($p_x > 0$) and the corresponding 3D perspective representation of the electron distribution function in the $p_x - v_y$ space (averaged over x variable) at the time $t\omega_p = 90$ at the end of the evolution. The most important feature is the appearance of a "beam" of accelerated particles at high energies which seems decoupled from the bulk of the plasma.

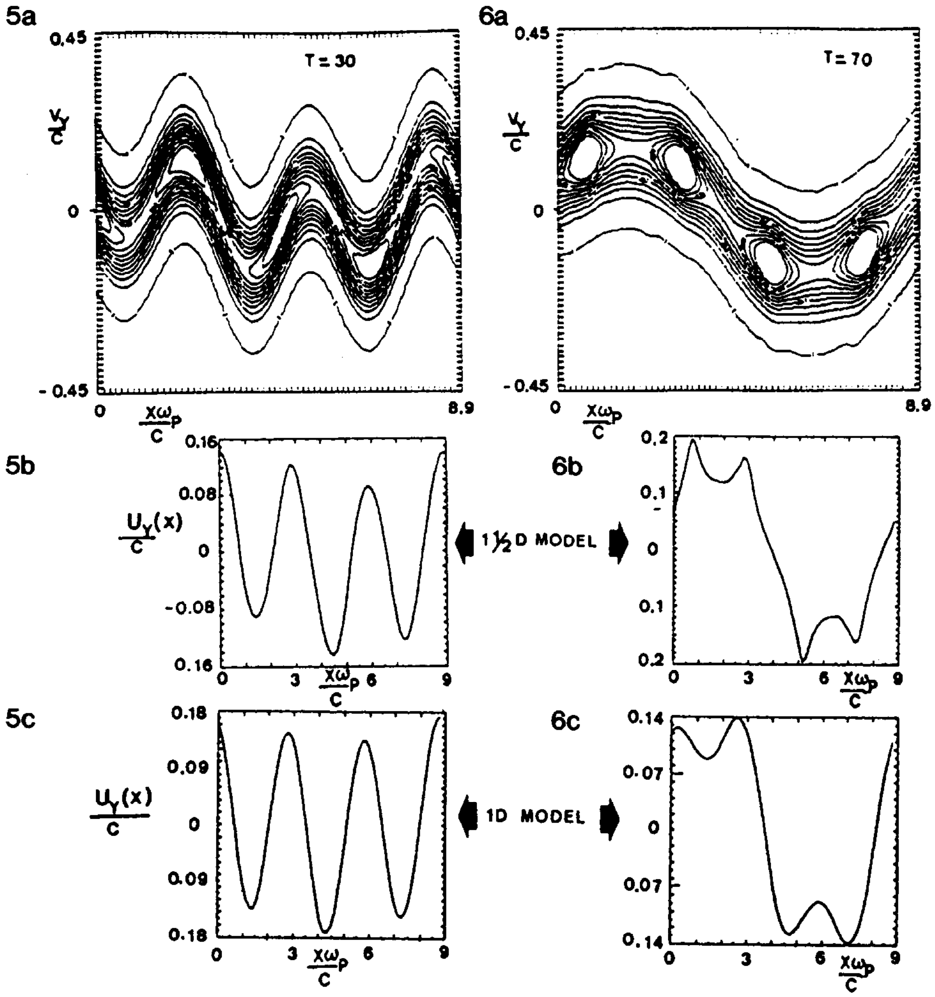

FIGS. 5, 6. For $t\omega_p = 30$ (Fig. 5) and $=70$ (Fig. 6): (a) phase-space $x - v_y$ for the $1\frac{1}{2}$D model; (b) mean velocity $u_y(y)$ for the $1\frac{1}{2}$D model corresponding to (a); (c) mean velocity $u_y(x)$ computed in the 1D model.

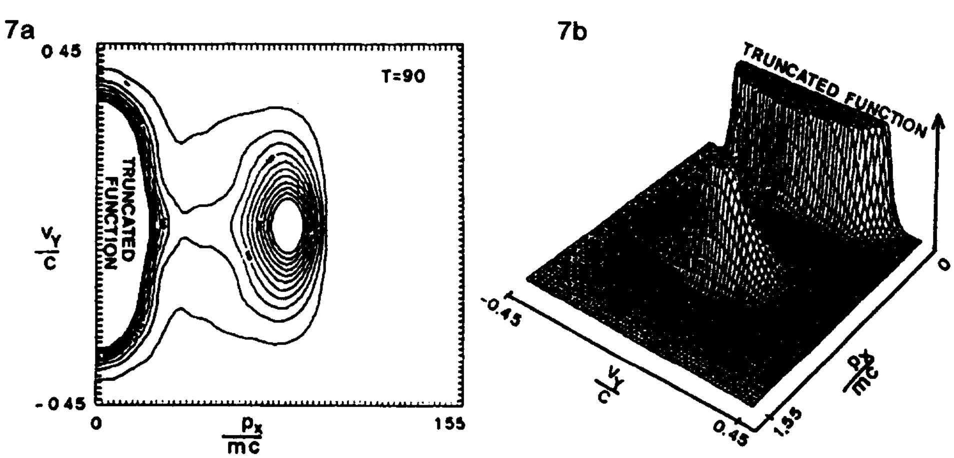

FIG. 7. Distribution function in the velocity space $(v_y p_x)$: (a) contour plot; (b) perspective view.

3. CONCLUSION

A $1\frac{1}{2}$D relativistic Euler–Vlasov code has been developed in order to check the validity of a hydrodynamical description used in a 1D version of the Vlasov code. Thus, detailed comparisons with numerical results obtained by using a 1D model have been carried out with those obtained with the $1\frac{1}{2}$D code. Good agreement provides full support for the 1D electromagnetic Vlasov code which runs considerably faster than the $1\frac{1}{2}$D code. Within the capacity of supercomputers, a full kinetic $1\frac{1}{2}$D code (i.e., 3D dimensional phase space) is now available and can be of great interest for some problems in the field of laser–plasma interaction. We note, however, that these results assume a non-relativistic v_y velocity.

ACKNOWLEDGMENTS

The Centre canadien de fusion magnétique is a joint venture of Hydro-Québec, Atomic Energy of Canada limited, and the Institut National de la recherche scientifique, in which MPB Technologies Inc., Canatom Inc., and the Université de Montréal also participate. It is principally funded by AECL, Hydro-Québec, and INRS.

REFERENCES

1. A. Ghizzo, P. Bertrand, M. Shoucri, T. W. Johnston, E. Filalkow, M. R. Feix, *J. Comput. Phys.* **90**, 431 (1990).
2. P. Bertrand, A. Ghizzo, T. W. Johnston, M. Shoucri, E. Fijalkow, M. R. Feix, *Phys. Fluids B* **2**, 1028 (1990).
3. P. Bertrand, A. Ghizzo, M. Shoucri, M. R. Feix, E. Fijalkow, T. W. Johnston, "A $1\frac{1}{2}$D Eulerian Vlasov code for the numerical simulation of the laser Beat-Wave interaction in a magnetized plasma," The 13th Conference on the Numerical Simulation of Plasmas, Santa Fe, New Mexico, September 1989, pp. 17–20, edited by Los Alamos National Laboratory, PMA 18.
4. C. Joshi, T. Tajima, and J. M. Dawson, *Phys. Rev. Lett.* **47**, 1287 (1981).
5. K. Estabrook, W. L. Kruer, and E. A. Williams, *Phys. Fluids* **31**, 372 (1988).
6. D. W. Forslund, J. M. Kindel, and E. L. Lindman, *Phys. Fluids* **18**, 1017 (1975).

Received August 1, 1990; revised August 6, 1991

A. Ghizzo
P. Bertrand
J. Lebas

Physique théorique, Université de Nancy-I
54506 Vandoeuvres-les-Nancy, France

M. Shoucri

Centre canadien de fusion magnétique
Varennes, Québec, Canada J3X 1S1

T. Johnston

INRS-Énergie, Varennes
Québec, Canada J3X 1S1

E. Fijalkow
M. R. Feix

P.M.M.S.–C.N.R.S.
45701 Orléans-la Source, France